Research Article

SURFACE and INTERFACE ANALYSIS

Received: 19 March 2009 Revised: 29 July 2009 Accepted: 24 August 2009 Published online in Wiley Interscience: 6 October 2009

(www.interscience.wiley.com) DOI 10.1002/sia.3116

Formation of alkane-phosphonic acid self-assembled monolayers on alumina: an *in situ* SPR study

Alexandros G. Koutsioubas,* Nikolaos Spiliopoulos, Dimitris L. Anastassopoulos, Alexandros A. Vradis and George D. Priftis

The formation process of *n*-alkane phosphonic acid CH_3 $(CH_2)_{n-1}$ $PO(OH)_2$ (n = 10,12,14,18) self-assembled monolayers (SAMs), deposited from ethanol solutions on aluminum oxide, has been monitored *in situ* using surface plasmon resonance (SPR) spectroscopy. In addition, the two-solvent approach is used to obtain both film thickness and refractive index of the fully formed adsorbed layers. A densely packed adsorbed layer is formed only for the longest molecules with n = 18. The chain length and solution concentration dependence of formation kinetics are studied, and the existence of two distinct kinetic steps is revealed. Fittings of the experimental results with various kinetic models are performed. Our analysis suggests that during the first kinetic step, a transition from a lying-down to a standing-up phase takes place, and the growth of this standing-up phase is governed by second-order kinetics. The second slow kinetic step is described by a modified first-order Langmuir law.

Keywords: surface plasmons; self-assembled monolayers (SAMs); aluminum; aluminum oxide; adsorption

Introduction

Self-assembled monolayers (SAMs) are ordered molecular assemblies formed by the adsorption of an active surfactant on a solid surface. SAMs have been the subject of many studies[1–3] in recent years due to their potential application in corrosion resistance, sensors, adhesion, lubrication, controlled surface patterning and in general the modification of surface properties. The simple fabrication process of SAMs as compared to the Langmuir-Blodgett films makes them quite attractive for technological applications.

In the last two decades, the most extensively studied SAM systems concern alkane-thiolates or dialkyl disulfides on gold[4–12] and silane-based molecules on various surfaces.[13–17] However, there is an increasing number of reports of SAMs based on organic acids such as alcanoic, sulfonic and phosphonic acids. It has been demonstrated[18–22] that these molecules can self-assemble on several metals or metal oxides, thus expanding the number and type of substrates that may be coated.

It is known for example[23] that phosphonic acids form monolayers on aluminum oxide (alumina – Al_2O_3) surfaces. As aluminum and its alloys find widespread applications in the aerospace, automotive, architectural and electronics sector, aluminum SAM coatings and their characterization are of great interest. Recently several reports[24–26] have addressed the equilibrium and formation properties of phosphonic acids on metal oxide surfaces by the use of various analytical techniques. These studies point out that for the metal oxide – phosphonic acid system, adsorption kinetics and total surface coverage are solvent dependent and that final film structure is strongly affected by chain length.

In the past, the entire range of surface sensitive experimental techniques has been used to probe the structural and dynamical properties of SAMs. *In situ* experimental studies using infrared spectroscopy,[7] surface plasmon resonance (SPR),[6] quartz crystal microbalance (QCM),[10] ellipsometry,[4,5,13,18–20] second harmonic generation (SHG),[12] atomic force microscopy (AFM)[14–17] may provide useful information in real time concerning the dynamics of formation of SAMs. On the other hand *ex situ* studies on quenched partial or complete monolayers permits the use of certain techniques that are not applicable *in situ*, such as x-ray reflectivity,[13] near edge x-ray adsorption fine structure spectroscopy (NEXAFS),[8,11] contact angle,[4,5,13,18–20,22] sum frequency generation (SFG)[27] and XPS.[11,13,21] The main advantage of *in situ* over *ex situ* studies is that SAM formation is probed under actual deposition conditions and implications associated with the quenching process are avoided.

The earliest kinetics experiments of SAM formation were carried by Bain *et al*.[5] for the adsorption of octadecanethiol from ethanol solutions on gold. Many studies have followed reporting contradictory results concerning adsorption rate constants, solvent effects and chain length dependence on the mechanisms of formation. Especially for the case of thiols on gold the reported rate constants of formation span over two orders of magnitude.[3]

Most of the above mentioned quantitative kinetic studies report a two-step mechanism for SAM formation, an initial fast step which is adequately described by Langmuir adsorption models and a second much slower step, leading to complete coverage. In an *in situ* AFM study[28] Doudevski *et al*. observed that the formation process of octadecyl-phosphonic acid SAMs on mica involves the nucleation of submonolayer islands that gradually grow and eventually coalesce. Based on this picture, Dannenbeeger

* *Correspondence to: Alexandros G. Koutsioubas, Physics Department, University of Patras, Patras 26500, Greece. E-mail: alexandk@physics.upatras.gr*

Physics Department, University of Patras, Patras 26500, Greece

et al.[12] proposed that the initial fast adsorption step is better described by a generalized model that takes into account different sticking probabilities for areas already covered and for those still free of thiols on a gold surface. For the case of phosphonic acids deposition from aqueous solutions onto aluminum oxide, Hauffman *et al.*[25] have reported the formation of multilayers, which is governed by a Stranski-Krastanov growth mechanism.

In this work, we present a detailed quantitative *in situ* kinetic study for the adsorption of *n*-alkane phosphonic acids ($n = 10,12,14,18$) onto alumina surfaces from ethanol solutions of varying concentration. By the excitation of surface plasmons (SPs) on thin aluminum films under the Kretchmann configuration, we have monitored in real-time the SAM adsorption process onto the native alumina layer that is present over the aluminum thin film. We observe the formation of a dense monolayer only for the longer chain length ($n = 18$) and two clearly distinct adsorption kinetics steps. Comparison of the experimental data with various kinetic models suggests that during the first kinetic step, two sequential processes take place, including the formation of a lying-down and a standing-up phase. It is also found that the second slow kinetic step is described by a modified first order Langmuir kinetic model.

Experimental

An extensive description of the SPR apparatus is given in a previous publication.[29] Briefly, we used a custom made SPR apparatus in the Kretschmann configuration. SPs are excited by a *p*-polarized laser beam ($\lambda = 632.8$ nm) on thin ($\sim$15 nm) aluminum films that are prepared by vacuum evaporation on the face of an optically flat SF10 high refractive index ($n_{SF10} = 1.7230$) equilateral prism. SAM formation is studied on the ultra-thin ($\sim$3 nm) naturally occurring oxide layer (alumina–Al_2O_3) that is formed on freshly evaporated aluminum films upon contact with the ambient. After each evaporation procedure the aluminum coated prisms were stored for at least 3 days in a specimen box left in the laboratory environment in order to ensure the complete formation of a stable oxide layer over the aluminum surface.

A custom made $\theta - 2\theta$ goniometer driven by two precision stepper motors was used to perform scans of the intensity of the reflected light as a function of the incidence angle (SPR curve). A beam splitter is placed between the laser source and the sample in order to monitor the source light intensity. The intensity of the source and reflected beams were measured with the aid of two photodiodes whose output was transmitted to a DSP module and on a PC for data processing and storage.

Ethanol solutions of four *n*-alkane phosphonic acids $CH_3(CH_2)_{n-1}PO(OH)_2$, where $n = 10,12,14,18$ (purchased from Alpha Aesar, Karlsruhe, Germany) were used in this study. Three different concentrations of 1 mM, 0.1 mM and 0.01 mM were prepared for the adsorption experiments. Solvent and solutions were injected in a custom made polytetrafluoroethylene (PTFE) cell which is sealed with the aid of a PTFE *O*-ring pressed against the aluminum coated face of the prism. The temperature inside the cell was monitored by a PTFE coated thermocouple. All measurements were performed at room temperature.

Analytical quality ethanol and heptane were purchased from Aldrich. All glassware that comes into contact with solvents and solution were cleaned by overnight exposure to fresh sulfochromic acid and then rinsed with deionized water and ethanol. The PTFE cell was cleaned by rinse with copious amounts of heptane and ethanol. At the beginning of each experiment the aluminum film SPR curve against air is measured. Then the PTFE cell is filled with ethanol and the aluminum/ethanol SPR curve was measured. The film formation experiments were initiated by forcing the desired solution into the cell and by acquiring SPR curves every 15 s for 1.5 h and every 10 min from this time on. After 20 h the cell is emptied and the film surface is thoroughly rinsed with heptane and ethanol. Then the cell is refilled with pure ethanol and the SPR curve is measured again *in situ*. Finally the cell is emptied, the SAM film is blown dry with nitrogen gas and the SPR curve is measured *ex situ* against air.

Data Analysis

In order to obtain the thickness of the partially formed SAM layers, the values of dielectric constants and thicknesses of the aluminum and alumina films obtained before solution injection were kept fixed. Fitting of the experimental data is performed under the matrix formalism for homogeneous stratified dielectric media and by the use of a five-layer model (SF-10 prism/aluminum/alumina/SAM layer/ethanol or air). The first and last layer is treated as semi-infinite. Each intermediate layer is characterized by its thickness and complex dielectric constant. Typical values of the calculated dielectric constants of aluminum and alumina were $\varepsilon_{Al} \sim -50 + i20$ and $\varepsilon_{Al_2O_3} = 2.8$ while the average thickness of the aluminum and alumina layer was 16 ± 0.5 nm and 3.1 ± 0.2 nm respectively. In all calculations the dielectric constant of ethanol is set according to the measured temperature using the value $dn_{ethanol}/dT = -0.0004/^{\circ}C$ for the refractive index temperature gradient.

The thickness of the SAM layer d_{SAM} is extracted from the fitting procedure by assuming that the dielectric constant of the SAM is equal to $\varepsilon_{SAM} = 2.21$. This value of ε_{SAM} was calculated by performing a two solvent experiment in ethanol and heptane, for a thoroughly rinsed fully formed octadecylphosphonic ($n = 18$) SAM (24 h adsorption). The two solvent approach permits the determination of both thickness and dielectric constant of a thin film.[6] The SPR curves for the two different solvents yield two different sets of ε_{SAM} and d_{SAM} pairs (Fig. 1). By assuming that the

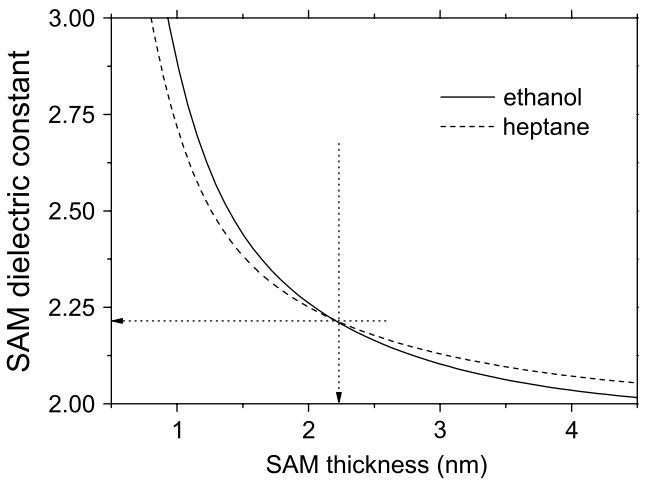

Figure 1. Two-solvent experiment for a octadecylphosphonic fully formed self-assembled monolayers (SAM). The two curves represent the dielectric constant – thickness pairs that are consistent with each measurement in ethanol and heptane. The intersection point yields the actual thickness (2.23 nm) and dielectric constant (2.21).

SURFACE and INTERFACE ANALYSIS

Table 1. Comparison of *in situ* (rinsed and unrinsed) and *ex situ* measured SAM thicknesses for adsorption from 1 mM ethanol solutions

n	*In situ* unrinsed (nm)	*In situ* rinsed (nm)	*Ex situ* rinsed (nm)	Theoretical (nm)
10	0.58	0.50	0.63	1.4
12	0.73	0.70	0.80	1.6
14	1.42	1.08	1.25	1.8
18	2.39	2.03	2.19	2.2

The last column contains the theoretical thickness of the SAM at full coverage by assuming that the molecular axes tilt 30° from the surface normal.

SAM structure is the same in both the solvents, the intersection point in Fig. 1, gives the actual ε_{SAM} and d_{SAM} pair. This procedure is necessary, as a single SPR measurement cannot yield a unique pair of dielectric constant and thickness of a thin (<20 nm) adsorbed film.[30] Note that for partially formed (sub-monolayer) films, the above described procedure yields the relative amount of adsorbed molecules per unit area (average film thickness).[6]

Uncertainties in the determination of SAM thickness are related to experimental errors in the acquired SPR curves that come mainly from the following sources: laser intensity fluctuations and noise in the photo detectors and related electronics, positioning uncertainty related to the limited accuracy of the goniometer and uncertainty related to the measured solution temperature. Calculations for the present experimental setup, summing up the contribution of all these error sources yields an accuracy of about ±0.05 nm in the determined SAM thickness.

Results and Discussion

The formation of $CH_3(CH_2)_{n-1}PO(OH)_2$ SAMs with $n = 10,12,14,18$ on alumina surfaces from ethanol solutions of three different concentrations 1 mM, 0.1 mM and 0.01 mM, was monitored over a period of 20 h. In Table 1, the final thickness that was measured *in situ* before and after film rinse and *ex situ* after film rinse is presented for adsorption from 1 mM solution. We observe that final film thickness is a monotonically ascending function of chain length *n*. As in the case of alkanethiols on gold,[6] thorough film rinse with ethanol and heptane leads to the removal of physi-adsorbed molecules. After solvent rinse, the *ex situ* measured thickness for all concentrations converge to the values presented in Table 1. However note that only for the longer molecules with $n = 18$, the final film thickness coincides with the theoretically expected value, assuming dense packing and that the molecular axes tilt 30° from the surface normal.

This fact suggests that for $n \leq 14$ the adsorbed layers are not characterized by a high crystallinity and that the chains are not in an all-trans conformation. This effect has been previously observed for phosphonic acid SAMs on titanium oxide surfaces[24] and has been attributed to the decrease of interchain van der Waals interactions for alkane chains of small molecular weight with $n \leq 14$.

In Fig. 2(a) and (b) the short and long time formation kinetics for 1 mM solution concentration are presented for all four molecules, while in Fig. 3(a) and (b) formation kinetics of octadecylphosphonic acid (ODP, $n = 18$) SAMs are illustrated for different solution concentrations. In all measurements we observe a fast first kinetic step that lasts for about 1200 s and a second much slower step that leads to final coverage. In the first step about 70–90% of the final coverage is achieved depending on the chain length studied.

Two distinct kinetic steps have also been previously reported in many studies for alkanethiols on gold[5,8] and various kinetic models have been proposed especially for the first step. Here, we attempted to fit the experimental results of the first step using five different kinetic models: (i) a first order Langmuir (LA) model, where film thickness dependence over time has the form $d(t) = d_0(1 - e^{-k_{LA}t})$; (ii) a diffusion-limited Langmuir model (DL),[6] where $d(t) = d_0(1 - e^{-k_{LD}\sqrt{t}})$; (iii) a non-diffusion limited second order Langmuir (SO) model,[6] where $d(t) = d_0[1 - (1 + k_{SO}t)^{-1}]$; (iv) a purely diffusion-controlled adsorption (DC) model $d(t) = k_{DC}t^{0.5}$; and (v) a modified Kisliuk (KM) model,[12] where $d(t) = d_0\left(\frac{e^{k_a(1+k_b)t} - 1}{e^{k_a(1+k_b)t} + k_b}\right)$

In LA, DL, SO and DC models k_{LA}, k_{DL}, k_{SO} and k_{DC} denote the characteristic growth rate parameter. The modified Kisliuk model that is motivated from the island growth picture, takes into account different sticking coefficients for areas already covered and for those still free. As the interaction of a molecule with a preformed island may be quite different from its interaction with the free surface, this deviation from first order Langmuir adsorption (LA) is incorporated by the rate constant k_b.

A least squares minimization routine was used in to determine the parameters (growth rates and d_0) of each model that better reproduce the experimental data. We have found that all experimental results for all combinations of solution concentration and chain length cannot be described by the DC and KM models (as a large mean of squared residuals is obtained by the fitting procedure), thus implying that simple chain diffusion or a model that assumes different sticking probabilities for covered and uncovered areas on the surface does not describe the SAM formation process as revealed by the present experimental data. Fittings of the first step kinetics with the other three models (LA, DL, SO) revealed that the second order Langmuir model (SO) gives the best fit. For example, in the case of ODP first step kinetics (Fig. 2) the fitting procedure gave a mean of squared residuals $\widehat{\chi^2}$ equal to 0.15 for the LA model, 0.35 for the DL model and 0.10 for the SO model.

In order to gain more insight into the ability of each model to describe the experimental data, we have adopted the following procedure. SAM thickness *versus* time is plotted in rescaled axes such that for the three models (LA, DL, SO) the experimental data should follow a straight line. The k_{LA}, k_{DL}, k_{SO} and d_0 values that were used to rescale the axes, were those found by the least squares minimization procedure. In Fig. 4, we illustrate the results of this procedure for ODP adsorption data, where it is obvious that the SO model is the most successful one in describing the data. However, we observe (Fig. 4(b)) that in the very early time of adsorption (60–100 s) there is a systematic deviation from the straight line until about 30% of the thickness d_0 is achieved, a feature that is more pronounced for $n = 18$. This deviation will be discussed in the following paragraphs.

At the microscopic level, in this first kinetic step of SAM formation, two processes are expected[3] to take place on the surface: (i) the rapid growth of a low-density lying-down phase where the molecular axes of the adsorbed molecules are parallel to the substrate and (ii) the transition from the lying-down to the dense standing-up phase where the molecular axes tilt ~30–45° from the surface normal. The second process, proceeds via the interaction of two molecules in order to form a new island nucleus or by the incorporation of a molecule at the boundary of an already

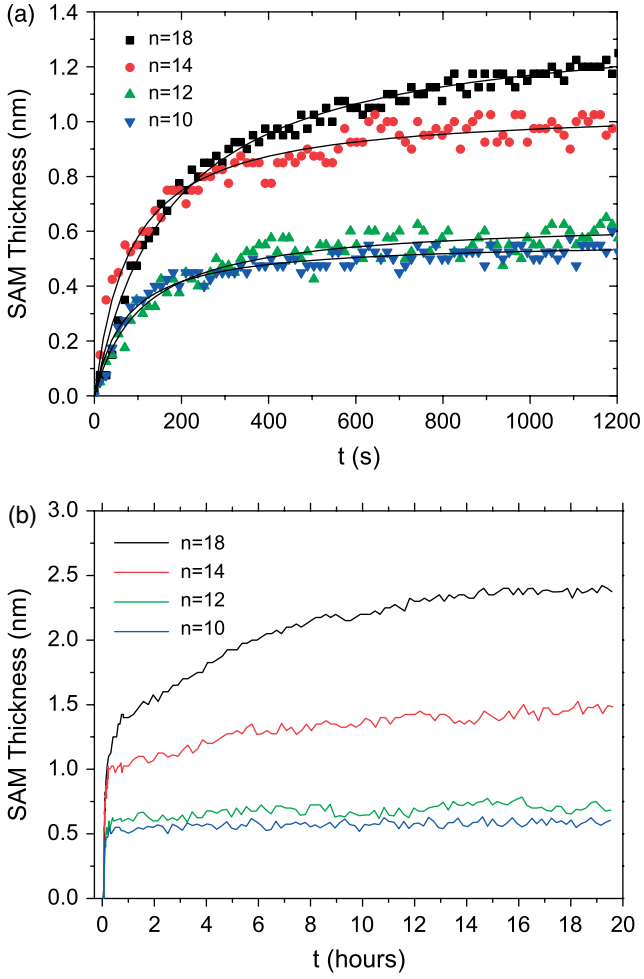

Figure 2. (a) Short time kinetics of SAM formation for all four molecules. Solution concentration is equal to 1 mM. Solid curves represent second order Langmuir (SO) fits to the experimental points. (b) Long time kinetics of SAM formation for all four molecules. Solution concentration is equal to 1 mM.

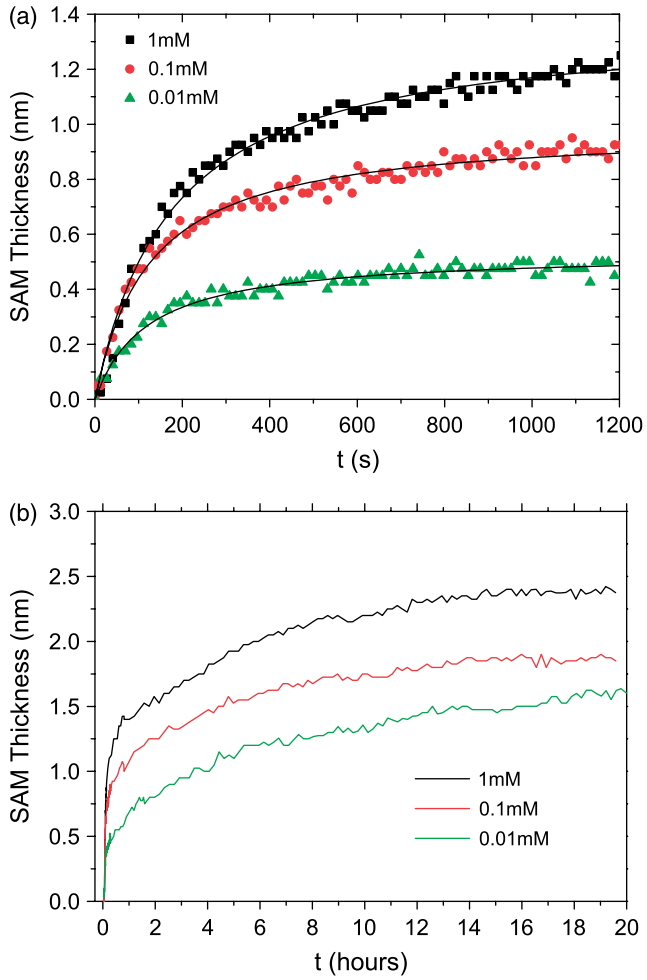

Figure 3. (a) Short time kinetics of octadecylphosphonic ($n = 18$) SAM formation for three different solution concentrations. Solid curves represent second order Langmuir (SO) fits to the experimental points. (b) Long time kinetics of octadecylphosphonic ($n = 18$) SAM formation for three different solution concentrations.

formed island. It has been found for thiol molecules[31] that the first rapid process obeys a first order Langmuir law, while the second process is described by a second order law.

By taking into account that the diameter of the alkane chains is equal to about 0.4 nm, we may assume that the lying-down phase represents about 20–30% of the fully formed SAM thickness, a fact that coincides with our observation that the second order law is accurately followed by the experimental points when about 30% of d_0 is achieved (Fig. 4(b)). This implies that strict second order behavior is observed after the formation of the lying-down phase. In order to clarify the validity of the fitting procedure, we have performed additional fits of the experimental points excluding those that are below the ~30% threshold of d_0 thickness. We found that the values of k_{LA}, k_{DL}, k_{SO} remain unchanged while the SO model gave the lower mean of squared residuals comparing to the other two models (LA, DL).

We argue that the observed second order kinetics and the calculated rate constants in our experimental data describe the growth of the standing-up phase which is essentially a second order – two molecule reaction on the surface. In previous investigations, only the early study of Peterlinz *et al.*[6] using SPR spectroscopy reported that second order kinetics governs the first kinetic step of thiol SAM formation on gold. Other studies[10,12] using different experimental techniques suggest that a first order Langmuir or a modified Kisliuk model better describes this first kinetic step. At this point, we have to note that surface analytical techniques such as SHG may be insensitive to the transition between the lying down and the standing-up phase in the first kinetic step, as their signal is determined by the number of chemical bonds that are formed on the surface. To some extent, these facts may be the reason for the different adsorption kinetics (LA, KM) observed using different experimental techniques. Probably the SFG technique (operated *in situ* whenever possible) is the most appropriate tool for such investigations of chain conformations during SAM formation.[27]

In Tables 2 and 3, we summarize the chain length and concentration dependence of the first-step rate constants that were obtained using LA and SO adsorption models. The SO rate constants (k_{SO}) found are of the same order of magnitude as those reported by Peterlinz[6] for thiol SAMs on gold. We note that while k_{SO} rate constants have an approximately linear descending relation *versus* chain length (Fig. 5), they are of the same order for all solution concentrations studied (Table 3). This fact indicates

SURFACE and INTERFACE ANALYSIS

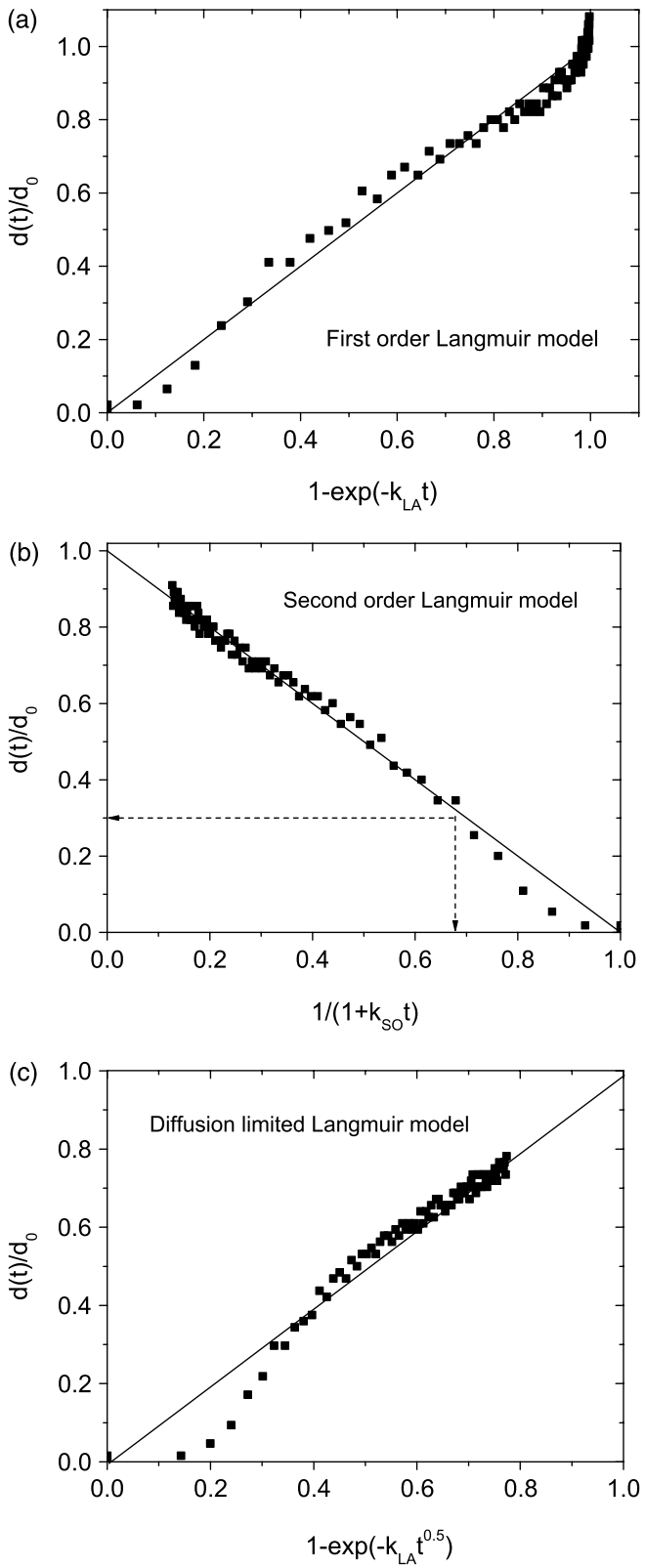

Figure 4. (a), (b) and (c). Short time kinetics of octadecylphosphonic (n = 18) SAM formation for 1 mM. solution concentration. Axes are rescaled so that for each kinetic model the experimental data should follow a straight line. Note that the second order model (b) is the more successful in describing the data points and that strict second order behavior is followed only after ~30% of the final adsorption is complete.

Table 2. Chain length dependence of SAM formation rate constants (ethanol solution concentration 1 mM)

	First kinetic step		Second kinetic step
n	LA k_{LA} (s^{-1})	SO k_{SO} (s^{-1})	k_{LT} (10^{-5} s^{-1})
10	0.0083 ± 0.0004	0.0146 ± 0.0009	0.5 ± 0.1
12	0.0070 ± 0.0004	0.0109 ± 0.0008	0.7 ± 0.1
14	0.0070 ± 0.0003	0.0097 ± 0.0005	1.4 ± 0.2
18	0.0049 ± 0.0001	0.0057 ± 0.0002	2.6 ± 0.2

LA rate constants are presented for the sake of comparison with other published works.

Table 3. Concentration (c) dependence of SAM formation rate constants (for octadecylphosphonic acid adsorption on alumina surfaces)

	First kinetic step		Second kinetic step
c	LA k_{LA} (s^{-1})	SO k_{SO} (s^{-1})	k_{LT} (10^{-5} s^{-1})
1 mM	0.0049 ± 0.0001	0.0057 ± 0.0002	2.6 ± 0.2
0.1 mM	0.0055 ± 0.0002	0.0068 ± 0.0003	2.6 ± 0.2
0.01 mM	0.0055 ± 0.0002	0.0071 ± 0.0004	2.4 ± 0.2

LA rate constants are presented for the sake of comparison with other published works.

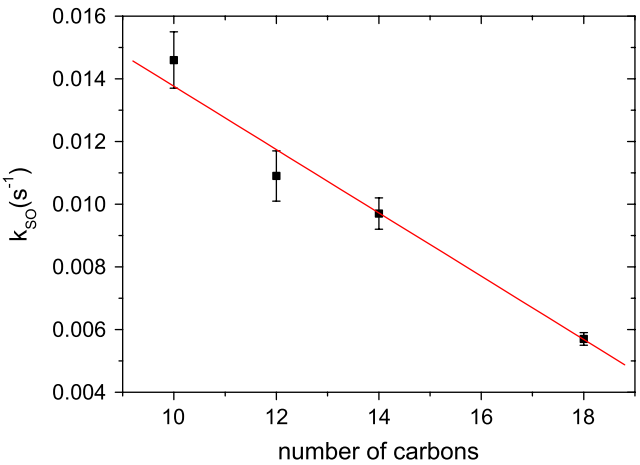

Figure 5. Second order Langmuir rate constant k_{SO} dependence on chain length n.

that the transition rate between the lying-down to the standing-up phase is primarily affected by chain length.

After the first step, a second much slower step is observed, that can be described by a modified first order Langmuir model of the form $d - d_{int} = d_{fin}(1 - e^{-k_{LT}t})$ where d_{fin} is the final SAM thickness and d_{int} the SAM thickness when the second kinetic step initiates. Fittings for this second step (Fig. 6) reveal that the relation of rate constant k_{LT} *versus* chain length n is opposite comparing to the results of the first step (Table 2) and that a linear descending relation between logk_{LT} versus n holds (Fig. 8). On the other hand, solution concentration has only a minor effect on k_{LT} (Fig. 7; Table 3) as in the case of the initial step. In this kinetic

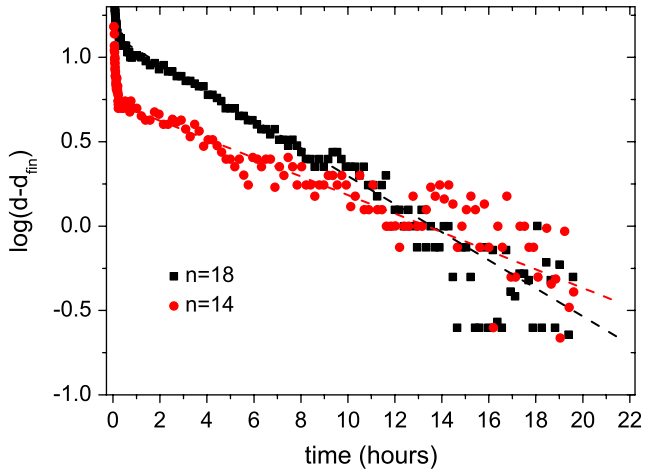

Figure 6. Semilog plot of SAM formation kinetics for solution concentration equal to 1 mM. After 30 min of adsorption a linear relation between $\log(d - d_{fin}) \sim t$ is established. The dashed lines represent linear fits to the experimental data (for $t > 0.5$ h).

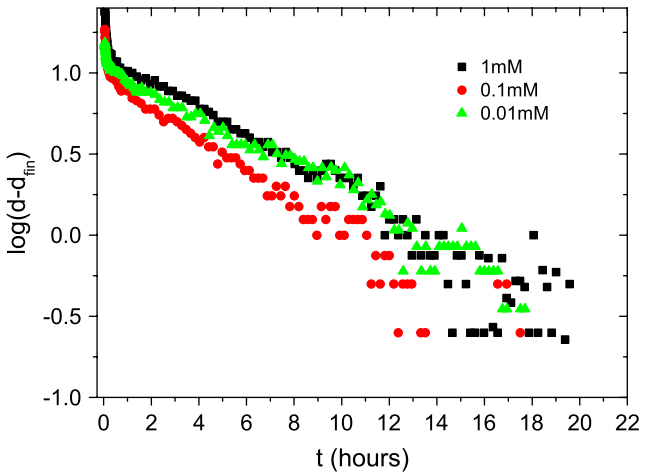

Figure 7. Semilog plot of octadecylphosphonic acid ($n = 18$) (SAM) formation kinetics for three different solution concentrations. Note that the slope for $t > 0.5$ h is almost concentration independent.

regime we expect that the main contribution comes from slow chain rearrangements that lead to island coalescence.

Based on the observation that solvent rinse, leads to a relative decrease of the layer thickness (especially for high solution concentrations), we may argue that in this late adsorption step, additional contribution to the measured layer thickness comes from physi-adsorbed molecules on top of the chemi-adsorbed layer. However, from the comparison of the measured values of layer thickness with the theoretical ones, (Table 1) the assumption of extensive multilayer formation as in the case of phosphonic acid SAM formation from aqueous solutions[25] is not favored.

Similar kinetic results have been published by Schwartz *et al.*[28] concerning octadecylphosphonic acid ($n = 18$) adsorption on mica. Although the used solvents and adsorbing surfaces are different between the two experiments, a qualitative comparison can be made. It is observed that the transition from the phase of island growth and aggregation to the phase of island coalescence, matches with the transition time between the two kinetic steps in

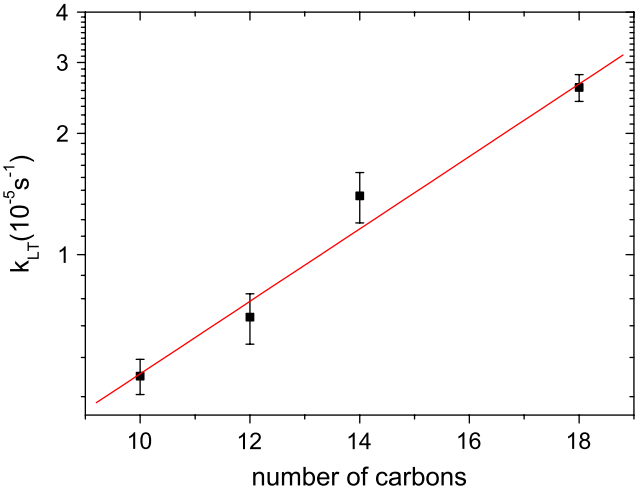

Figure 8. Second kinetic step rate constant k_{LT} dependence on chain length n.

our experiments. This fact indicates that in both cases the same mechanism of island formation and growth is at play.

A final remark, we would like to make, concerns the potential use of the SPR method in corrosion studies.[32] Recently the dynamic contact angle (DCA) technique has been implemented for the study of the aqueous stability of alkyl-phosphonic and alkyl-carboxylic SAMs on alumina.[33] The present experimental setup (i.e. aluminum film based SPR) may find use in the study of SAM induced corrosion resistance of aluminum in acidic environments. By exposure of the SAM coated aluminum film to a solution of high or low pH, one may monitor *in situ* the SPR curve over time and relate the observed changes to SAM degradation and/or aluminum thin film corrosion.

Conclusions

In situ aluminum film based SPR studies on the adsorption of alkane-phosphonic acid from ethanol solution onto alumina have been performed. We have found that dense monolayers are formed only for chains with more than 14 carbons. Adsorption takes place in two main steps and the film final thickness is an ascending function of chain length. The analysis of adsorption kinetics indicates that during the first step, two processes take place on the surface, i.e. the fast formation of a lying-down phase and a subsequent transition to the dense standing-up phase which is governed by second order kinetics. The second much slower step is described by a modified first order Langmuir model. In both kinetic steps, rate constants are primarily affected by the number of carbons of the chains. Finally, we also propose that apart from SAM formation studies, aluminum based SPR may be used in corrosion resistance studies. Future work will focus on such applications.

References

[1] A. Ulman, *Chem. Rev.* **1996**, *96*, 1533.
[2] F. Schreiber, *Prog. Surf. Sci.* **2000**, *65*, 151.
[3] D. K. Schwartz, *Annu. Rev. Phys. Chem.* **2001**, *52*, 107.
[4] R. G. Nuzzo, D. L. Allara, *J. Am. Chem. Soc.* **1983**, *15*, 4481.
[5] C. D. Bain, E. B. Troughton, Y. Tao, J. Evall, G. M. Whitesides, R. G. Nuzzo, *J. Am. Chem. Soc.* **1989**, *111*, 321.
[6] K. A. Peterlinz, R. Georgiadis, *Langmuir* **1996**, *12*, 4740.

[7] D. S. Karpovic, G. J. Blanchard, *Langmuir* **1994**, *10*, 3315.
[8] G. Hahner, Ch. Woll, M. Buck, M. Grunze, *Langmuir* **1993**, *9*, 1955.
[9] K. D. Truong, P. A. Rowntree, *Prog. Surf. Sci.* **1995**, *50*, 207.
[10] Y. T. Kim, R. L. McCarley, A. J. Bard, *Langmuir* **1993**, *9*, 1941.
[11] O. Dannenberger, K. Weiss, H. Himmel, B. Jager, M. Buck, C. Woll, *Thin Solid Films* **1997**, *307*, 183.
[12] O. Dannenberger, M. Buck, M. Grunze, *J. Phys. Chem. B.* **1999**, *103*, 2202.
[13] S. R. Wasserman, G. M. Whitesides, I. M. Tidswell, B. M. Ocko, P. S. Pershan, J. D. Axe, *J. Am. Chem. Soc.* **1989**, *111*, 5852.
[14] D. K. Swartz, S. Steinberg, J. Israelachvili, J. A. N. Zasadzinski, *Phys. Rev. Lett.* **1992**, *69*, 3354.
[15] K. Bierbaum, M. Grunze, A. A. Baski, L. F. Chi, W. Schrepp, H. Fuchs, *Langmuir* **1995**, *11*, 2143.
[16] B. L. Kropman, D. H. A. Blank, H. Rogalla, *Thin Solid Films* **1998**, *327-329*, 185.
[17] M. Goldmann, J. V. Davidovits, P. Silberzan, *Thin Solid Films* **1998**, *327*, 166.
[18] D. L. Allara, R. G. Nuzzo, *Langmuir* **1985**, *1*, 45.
[19] D. L. Allara, R. G. Nuzzo, *Langmuir* **1985**, *1*, 52.
[20] M. J. Pellerite, T. D. Dunbar, L. D. Boardman, E. J. Wood, *J. Phys. Chem. B* **2003**, *107*, 11726.
[21] I. L. Liakos, R. C. Newman, E. McAlpine, M. R. Alexander, *Surf. Interface Anal.* **2007**, *36*, 347.
[22] K. M. Pertays, G. E. Thompson, M. R. Alexander, *Surf. Interface Anal.* **2004**, *36*, 1361.
[23] E. Hoque, J. A. DeRose, P. Hoffmann, H. J. Mathieu, B. Bhushan, M. Cichomsko, *J. Chem. Phys.* **2006**, *124*, 174710.
[24] D. M. Spori, N. V. Venkataraman, S. G. P. Tosatti, F. Durmaz, N. D. Spencer, S. Zurcher, *Langmuir* **2007**, *23*, 8053.
[25] T. Hauffman, O. Blajiev, J. Snauwaert, C. van Haesendonck, A. Hubin, H. Terryn, *Langmuir* **2008**, *24*, 13450.
[26] T. A. Lewington, M. R. Alexander, G. E. Thompson, E. Mcalpine, *Surf. Eng.* **2002**, *18*, 228.
[27] M. Himmelhaus, F. Eisert, M. Buck, M. Grunze, *J. Phys. Chem. B* **2000**, *104*, 576.
[28] I. Doudevski, W. A. Hayes, D. K. Schwartz, *Phys. Rev. Lett.* **1998**, *81*, 4927.
[29] A. G. Koutsioubas, N. Spiliopoulos, D. L. Anastassopoulos, A. A. Vradis, C. Toprakcioglu, G. D. Priftis, *J. Polym. Sci. Part B: Polym. Phys.* **2006**, *44*, 1580.
[30] A. G. Koutsioubas, N. Spiliopoulos, D. L. Anastassopoulos, A. A. Vradis, G. D. Priftis, *J. Polym. Sci. Part B: Polym. Phys.* **2007**, *45*, 2060.
[31] S. Xu, S. J. N. Cruchon-Dupeyrat, J. C. Garno, G. Y. Liu, G. K. Jennings, T.-H. Yong, P. E. Laibinis *J. Chem. Phys.* **1998**, *108*, 5002.
[32] R. J. Busshager, H. A. Macleod, *Appl. Opt.* **1996**, *35*, 5044.
[33] I. L. Liakos, R. C. Newman, E. McAlpine, M. R. Alexander, *Langmuir* **2007**, *23*, 995.

